Catalysis Today 283 (2017) 11–26

Contents lists available at ScienceDirect

Catalysis Today

journal homepage: www.elsevier.com/locate/cattod

Twenty years of operando IR, X-ray absorption, and Raman spectroscopy: Direct methanol and hydrogen fuel cells

Neili Loupe, Jonathan Doan, Eugene S. Smotkin*

Department of Chemistry and Chemical Biology, Northeastern University, Boston MA 02115, United States

ARTICLE INFO

Article history:
Received 14 December 2015
Received in revised form 1 June 2016
Accepted 4 June 2016
Available online 20 June 2016

Keywords:
Operando spectroscopy
X-ray absorption spectroscopy
Infrared spectroscopy
Raman spectroscopy

ABSTRACT

Mixed metal catalysts in polymer electrolyte fuel cell membrane electrode assemblies were characterized by operando infrared, X-ray absorption and Raman spectroscopy. Windowed direct methanol and hydrogen-air fuel cell assemblies allow for spectral acquisition with controlled potential, temperature and flowing reactant streams to the graphite flow fields. Johnson Matthey Pt and PtRu (1:1), in-house prepared PtRu (1:1 and 3:1), PtRuOs (65:25:10), PtNi (1:1), and a melamine-synthesized FeNC catalyst were studied. The near invariant core structure of phase segregated alloy catalysts over practical fuel cell potentials enable a simultaneous fit of metal component EXAFS to quantitatively characterize core structures: JM PtRu is a face centered cubic lattice with 50% of the Ru in an amorphous phase. Stark tuning of CO_{ads} as a reaction intermediate and as a surface structure probe elucidates potential dependent co-adsorption of Nafion functional groups on Pt. Operando Raman spectroscopic tracking of membrane hydration at a fuel cathode is facilitated by symmetry-based group mode assignments of Nafion IR bands. Fully hydrated Nafion sulfonate groups have C_{3V} local symmetry. Dehydrated sulfonic acid groups have C_1 local symmetry. C_{3V} and C_1 IR bands coexist at intermediate states of membrane hydration.

1. Introduction

1.1. Polymer electrolyte membrane fuel cells

Polymer electrolyte membrane (PEM) fuel cells are ideal for portable, traction and stationary power. This perspective summarizes our studies, since 1996, of direct methanol fuel cell (DMFC) and hydrogen-air fuel cell electrode layers, with an emphasis on operando spectroscopy [1–14].

Fig. 1 schematizes a fuel cell and the electrocatalytic layer structure. The membrane electrode assembly (MEA) is a Nafion membrane sandwiched between anode and cathode catalytic layers. A fuel (e.g., MeOH or H_2) is oxidized at the anode and air (or O_2) is reduced at the cathode. The hydrogen-air fuel cell anode and cathode half reactions are:

$$H_2 \rightarrow 2H^+ + 2e^- \quad (1)$$

$$O_2 + 4e^- + 4H^+ \rightarrow 2H_2O \quad (2)$$

Catalytic layers are formed by deposition of catalyst inks upon porous carbon paper/cloth gas diffusion layer (GDL) surfaces. The GDLs are both current collectors and diffusers for gaseous or reactants between the flow fields and catalytic layers. Teflon dispersion in the cathode layer rejects water from the oxygen reduction reaction (ORR). The solubilized Nafion component of catalyst inks [15] imparts proton conductivity throughout the catalytic layer. Catalyzed GDLs are hot pressed onto Nafion to yield a 5-layer MEA. Catalyst inks can also be directly applied to the membrane to yield a catalyst coated membrane (CCM). MEA fabrication methods are reviewed by Gottesfeld [16].

Ideally, PEM fuel cells will tolerate direct oxidation of liquid fuels (e.g., MeOH) and/or H_2 derived from hydrocarbon reformation (with typically 50–100 ppm CO). In either case, adsorbed CO (CO_{ads}) blocks active catalytic sites for MeOH or H_2 oxidation. Pt has been the standard anode catalyst with the best performance of all pure metals [18]. The best-known CO tolerant catalysts are Pt-based mixed metal catalysts [3].

1.2. DMFC and hydrogen-air fuel cell catalysis

Condensed MeOH has five times the energy density of compressed H_2 [19]. Unlike H_2 fuel cells, DMFCs can leverage an existing liquid fuel infrastructure. Improved catalysts for the MeOH half-reaction (Eq. (3)) would obviate the need for the reformer,

---

* Corresponding author.
E-mail address: e.smotkin@neu.edu (E.S. Smotkin).

http://dx.doi.org/10.1016/j.cattod.2016.06.012

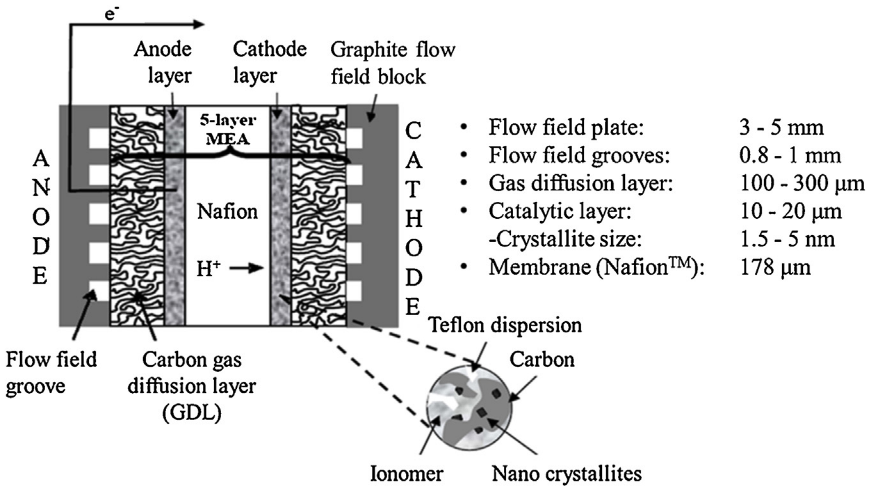

Fig. 1. Polymer electrolyte membrane fuel cell with a 5-layer membrane electrode assembly. Inset shows cathode catalytic layer structure. Adapted from Ref. [17].

water-gas-shift reactor and preferential oxidation units required for production of pure H_2.

$$CH_3OH + H_2O \rightarrow CO_2 + 6H^+ + 6e^- \tag{3}$$

Gilman proposed the mechanism for methanol electro-oxidation on Pt [20]. “Bifunctional theory” was coined to apply Gilman’s reaction pair concept to Pt-rich alloy catalysts for MeOH oxidation [21]. The following is a modification of Gilman’s mechanism by Frelink et al [22] and Watanabe and Motoo [23] (alloying component, or promoter metal, is represented as M):

$$\text{Pt} + CH_3OH \rightarrow \text{Pt-}(CH_3OH)_{ads} \tag{4}$$

$$\text{Pt-}(CH_3OH)_{act} \rightarrow \text{Pt-}(CH_3O)_{act} + H^+ + e^- \tag{5a}$$

$$\text{Pt-}(CH_3O)_{act} \rightarrow \text{Pt-}(CH_2O)_{act} + H^+ + e^- \tag{5b}$$

$$\text{Pt-}(CH_2O)_{act} \rightarrow \text{Pt-}(CHO)_{act} + H^+ + e^- \tag{5c}$$

$$\text{Pt-}(CHO)_{act} \rightarrow \text{Pt-}(CO)_{act} + H^+ + e^- \tag{5d}$$

$$M + H_2O \rightarrow M\text{-}(H_2O)_{act} \tag{6}$$

$$\text{Pt-}(CO)_{ads} + M\text{-}(H_2O)_{act} \rightarrow \text{Pt} + M + CO_2 + 2H^+ + 2e^- \tag{7}$$

Within practical DMFC anode potentials (<300 mV vs. Reversible Hydrogen Electrode (RHE)) the rate determining step (RDS) on pure Pt is water activation (Eq. (6)). Deuterium isotope studies confirm that at 350–400 mV, the RDS on PtRu shifts from water activation to the first C—H activation step (Eq. (5a)) [24] Ru, as a promotor metal, shifts water activation by over 200 mV vs. Pt (Fig. 2). The state-of-the-art DMFC catalyst is Johnson Matthey (JM) unsupported PtRu (1:1).

Pt alloying also benefits reformate hydrogen fuel cells. Reformate hydrogen electrocatalysis is distinctly different from that of DMFCs, where CO is a reaction intermediate that must be oxidized if all six electrons in the MeOH oxidation half reaction are to be realized (Eq. (3)). When reformate H_2 is used, CO cumulatively poisons active sites. Since the hydrogen anode potential is never sufficiently positive to oxidize CO, the more important issue to reformate H_2 fuel cells is the ligand effect: The reduction of the CO adsorption enthalpy by alloying Pt with promoter metals improves hydrogen competitive adsorption on active sites [22,25].

Frelink [22] presents the ligand effect as an alloy electronic effect that impacts the Pt-C bond strength, while Nørskov [25] explains it in terms of d-band center shifting. Our DFT results attribute the ligand effects to a d-band dispersion mechanism [26] With DMFCs the bifunctional mechanism is essential because, in contrast to reformate fuel cells, the CO must be electrooxidized.

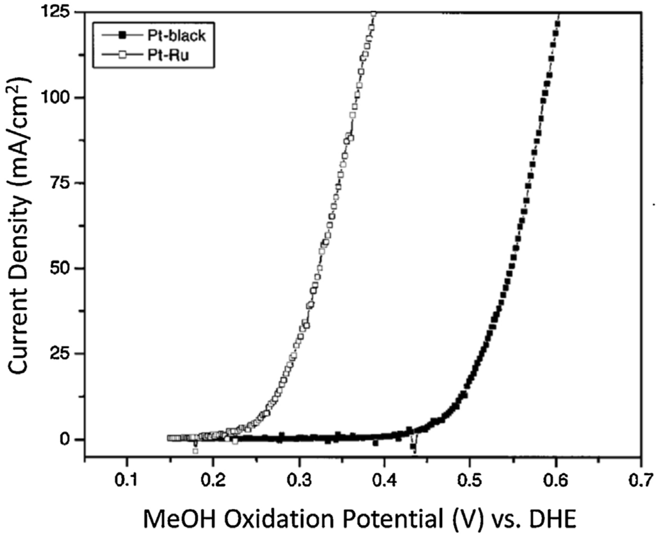

Fig. 2. Steady-state MeOH polarization curves; JM Pt and JM PtRu (1:1). Adapted from Ref. [5].

1.3. *Stark tuning of CO_{ads}*

The variation of vibrational band frequencies with electrode potential is Stark tuning [27,28]. In a model describing the interaction between the CO molecule and Pt d states, Nørskov describes the bonding in two steps (Fig. 3) [25,29]. In the first step, the $2\pi^*$ and the 5σ MOs are shifted down in energy and broadened due to coupling with the Pt s,p electrons. The renormalized CO orbitals are then mixed with the Pt d-band resulting in the splitting of the $2\pi^*$ MO into Pt-C antibonding and bonding orbitals.

Thus as the electrode potential is increased, the Pt-C π-bonding orbital (derived in part from the CO $2\pi^*$ molecular orbital) is depopulated. This increases the C—O bond order concomitant with the stretching frequency (i.e., Stark tuning). A second factor is dipole-dipole coupling where stretching frequencies increase with surface coverage, or compression of existing coverage by co-adsorbates. This phenomena is due to increased spatial dipole-dipole interactions via coupling through metal electrons [30–34]. Oxidation of